

One-dimensional Lévy Quasicrystal

Pallabi Chatterjee^{1,*} and Ranjan Modak^{1,†}

¹*Department of Physics, Indian Institute of Technology Tirupati, Tirupati, India 517619*

Space-fractional quantum mechanics (SFQM) is a generalization of the standard quantum mechanics when the Brownian trajectories in Feynman path integrals are replaced by Lévy flights. We introduce Lévy quasicrystal by discretizing the space-fractional Schrödinger equation using the Grünwald-Letnikov derivatives and adding on-site quasiperiodic potential. The discretized version of the usual Schrödinger equation maps to the Aubry-André Hamiltonian, which supports localization-delocalization transition even in one dimension. We find the similarities between Lévy quasicrystal and the Aubry-André (AA) model with power-law hopping, and show that the Lévy quasicrystal supports a delocalization-localization transition as one tunes the quasiperiodic potential strength and shows the coexistence of localized and delocalized states separated by mobility edge. Hence, a possible realization of SFQM in optical experiments should be a new experimental platform to test the predictions of AA models in the presence of power-law hopping.

I. INTRODUCTION

In usual quantum mechanics, the typical energy-momentum relation for a particle of mass m is given by $E = P^2/2m$. In general, one can have a situation where the energy-momentum relation is given by $E \propto P^{\alpha}$, where α can be a fraction. This kind of situation can be described by the Space Fractional Quantum Mechanics (SFQM), which was introduced by Laskin²⁻⁷. SFQM is a natural generalization of the standard quantum mechanics that arises when the Brownian trajectories in Feynman path integrals are replaced by Lévy flights. The classical Lévy flight is a stochastic process that, in one dimension is described by a jump length probability density function (PDF) of the form, $\Pi_{\alpha}(x) \propto 1/|x|^{\alpha+1}$ for $|x| \rightarrow \infty$, with $\alpha \in (0, 2]$ ⁵, where α is known as Lévy index.

There have been numerous applications of classical Lévy flights. Especially, in the context of successfully predicting the anomalous scaling of dynamical correlations of conserved quantities in one-dimensional (1D) Hamiltonian systems, the Lévy scaling for the spreading of local energy perturbation has been predicted, as well as diverging thermal conductivity (via GreenKubo formula)⁸⁻¹¹. Also, in order to understand the motion of the particle in a rotating flow^{12,13} or even the traveling behavior of animals¹⁴⁻¹⁷, the complex dynamics of real-life financial markets¹⁸, Lévy description has been extremely useful. It has been shown recently in Ref.⁵, one can discretize Space fractional Schrödinger equation, introduce a system which is referred to as Lévy Crystal. Given the extraordinary advancements of ultra-cold experiments in the last two decades, Lévy Crystal is a potential candidate for an experimentally accessible realization of SFQM in a condensed-matter environment¹⁹⁻²¹, however, it has not been explicitly demonstrated how that can be achieved in Ref.⁵. Moreover, fractional quantum mechanics plays a very crucial role in optical systems²²⁻²⁷. In this context, there have been recent theoretical works on domain walls in fractional media²⁸, fractional diffraction in the context of parity-time symmetric poten-

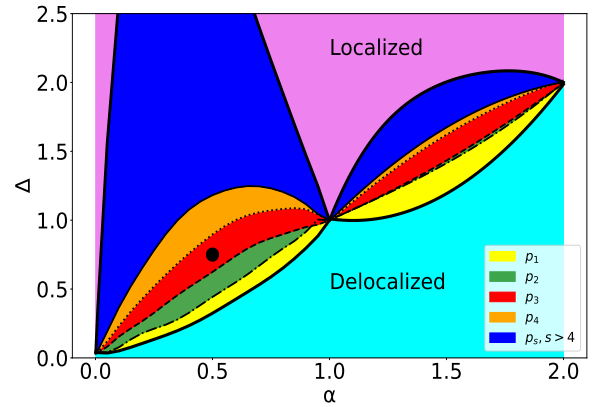


FIG. 1. Here we show the phase diagram of the Lévy quasicrystal. Black circle represents $\alpha = 0.5$ and $\Delta = 0.75$. In the main text, we show the results corresponding to this point.

tials²⁹⁻³¹, and on optical solitons³²⁻⁵⁴, that brought lots of attention. The experimental realization of an optical system representing the fractional Schrödinger equation has been reported very recently in Ref.⁵⁵. Also, it is important to point out that in the context of Sisyphus cooling, fractional equations arise from the dynamics of cold atoms, an effect that is well-studied^{56,57}.

On the other hand, the disorder is ubiquitous in nature, and in the condensed matter system, it plays a very important role. In the one-dimensional (1D) system, the disorder has an extreme consequence, even a tiny bit of disorder is sufficient to localize all the single-particle states. This phenomenon is famously known as Anderson localization⁵⁸⁻⁶⁰. In recent days, there has been a plethora of work to understand the interplay of interaction and disorder, and that cause a delocalization-localization transition in the many-body Fock space, which is referred to as many-body localization (MBL) transition^{20,61-65}. In the experimental point of view, realizing true disorder in ultra-cold experiments is non-trivial, hence one of the obvious candidates is to replace it with the quasiperiodic

potential. In contrast to the true disorder, quasiperiodic potential can cause a delocalization-localization transition in 1D even in the absence of interaction, and this Hamiltonian is known as Aubry-André (AA) model⁶⁶. While the nature of the localized phase observed due to quasiperiodic potentials and true disorders are the same (in both cases, eigenstates are exponentially localized), there are differences in critical properties associated with the localization-delocalization transition. In both cases, the localization length ξ diverges at the transition following as $\xi \sim \delta^{-\nu}$, where δ is the distance to the critical point in the parameter space and ν is the localization length exponent. In true disorder-driven localization, there is a rigorous bound on the localization length exponent ν , i.e., it must satisfy $\nu \geq 2/d$ criteria to ensure the stability of the transition⁶⁷. However, in quasiperiodic models, such criteria do not apply. For most of the one-dimensional quasi-periodic models, ν is close to 1⁶⁸. In recent days, there have been numerous studies, both theoretically and experimentally, involving a variant of the AA model that shows the coexistence of both localized and delocalized states separated by a mobility edge^{69–83}.

In this work, one of the main aims is to address the question of what happens to the fate of Anderson localization in the context of SFQM in the presence of quasiperiodic potential, we call it Lévy quasicrystal. Interestingly, a similar question has been asked in a recent study²⁶, but a detailed theoretical understanding of the phase diagram of the different phases was lacking there. Also, the Lévy-flight models have been used extensively in understanding real-life financial markets, the traveling behavior of humans, and even biological systems. If one wants to model such a system and take into account correlated random events, our Lévy quasicrystal model can be an extremely suitable candidate for such cases. We demonstrate the phase diagram as a function of α and the strength of the quasiperiodic potential Δ , which is shown in Fig. 1. While we find that like the Aubry-André model (which is the discretized version of the usual Schrödinger equation), there exists a completely delocalized (DL) and Anderson localized (AL) phase, but on top of that there is a parameter region where these two types of states coexist, and they are separated by the mobility edge (ME). Those ME phases can also be characterized as different p_s phases (where $s > 0$ can be any positive integer) based on the fraction of delocalized states in the spectrum. We also compare our model with a potential experimentally realizable AA model with power-law hopping.

The paper is organized as follows. In Sec. II, we introduce the model of Lévy quasicrystal. Next, we discuss the analytical prediction of the mobility edge in Sec. III. In Sec. IV, we show our numerical results. Sec. V shows the comparison between Lévy quasicrystal and the effective power-law hopping model and finally, we summarize our results in Sec. VI.

II. MODEL

The one-dimensional space-fractional Schrödinger equation is given by,

$$H|\psi\rangle = D_\alpha P^\alpha |\psi\rangle + V|\psi\rangle = E|\psi\rangle, \quad (1)$$

where $D_\alpha \in \mathbb{R}$ is a constant (note that D_2 is equivalent of inverse of mass term in usual Schrödinger equation), P^α is the α -th power of the momentum operator, V is the potential energy operator and $|\psi\rangle$ is the eigenstate with eigenvalue E ^{2,3,5}.

The position space representation of α -th power of the momentum operator is $\langle x|P^\alpha|\psi\rangle = -\hbar^\alpha \mathcal{D}_{|x|}^\alpha \psi(x)$ ^{4,5}, where $\mathcal{D}_{|x|}^\alpha$ is the Riesz Fractional Derivative of order α . While usually to get the finite first moment of the Lévy process, α is taken within the limit $\alpha \in (1, 2]$ ⁴, but given there exist, biological models, where the Lévy parameter is taken to be $0 < \alpha < 1$ ¹⁵, also in a very recent optical experiment, the parameter range $\alpha < 1$ of the fractional Schrödinger equation has been realized⁵⁵ in the temporal domain, that motivates us to even explore the extended parameter regime, and we use the same position space representation of α -th power of the momentum operator for $\alpha \in (0, 2]$ to get the discretized version. Riesz Fractional Derivative of order α (note that we consider $\alpha = 1$ point separately in the appendix), can be written as^{5,84} (note that the expression of the Riesz Fractional Derivative is taken from Ref.⁸⁴),

$$\mathcal{D}_{|x|}^\alpha = -\frac{1}{2 \cos(\frac{\alpha\pi}{2})} (I_+^{-\alpha} + I_-^{-\alpha}), \quad (2)$$

where $I_\pm^{-\alpha}$ are given by (approximating Grünwald-Letnikov operators)^{5,84},

$$I_\pm^{-\alpha} \psi(x) = \lim_{a \rightarrow 0} \frac{1}{a^\alpha} \sum_{n=0}^{\infty} (-1)^n \binom{\alpha}{n} \psi[x \mp an], \quad (3)$$

for $0 < \alpha \leq 1$.

$$I_\pm^{-\alpha} \psi(x) = \lim_{a \rightarrow 0} \frac{1}{a^\alpha} \sum_{n=0}^{\infty} (-1)^n \binom{\alpha}{n} \psi[x \mp (n-1)a], \quad (4)$$

for $1 < \alpha \leq 2$. Where a stands for a small positive step length. Here, $\binom{\alpha}{n} = \frac{\Gamma(\alpha+1)}{\Gamma(n+1)\Gamma(\alpha-n+1)}$, where $\Gamma(\cdot)$ is the usual Gamma function. It is straightforward to check that for $\alpha = 2$ Riesz Fractional Derivative becomes the standard second-order derivative.

In this work, we consider the potential to be space-dependent (quasiperiodic potential), hence the model can be represented by the equation,

$$\langle x_l | H | \psi \rangle = \langle x_l | D_\alpha P^\alpha | \psi \rangle + \Delta \cos(2\pi\beta l + \phi) \psi(x_l). \quad (5)$$

x_l is equally spaced grid points i.e $x_l = la$, a =lattice constant, $a > 0$ and $l \in \mathbb{Z}$. β is an irrational number.

We choose $\beta = \frac{\sqrt{5}-1}{2}$, and ϕ is a random number chosen between $[0, 2\pi]$. Note that in the previous study⁵ the potential energy term was considered to be periodic in lattice spacing a , the construction of the space-fractional Schrödinger equation via Riesz Fractional Derivative is not only limited to periodic potential.

Replacing the exact momentum operator by its discretized version^{5,85} and using Eqn. (4), one gets for $1 < \alpha \leq 2$,

$$\langle x_l | D_\alpha P^\alpha | \psi \rangle := \frac{t_0}{2} \sum_{n=0}^{\infty} (-1)^n \binom{\alpha}{n} (\psi[x_l + (n-1)a] + \psi[x_l - (n-1)a]), \quad (6)$$

where $t_0 = \frac{D_\alpha \hbar^\alpha}{a^\alpha \cos(\frac{\alpha\pi}{2})}$.

Then, $\langle x_l | D_\alpha P^\alpha | \psi \rangle$ becomes,

$$\begin{aligned} \langle x_l | D_\alpha P^\alpha | \psi \rangle := & \\ & \frac{t_0}{2} \sum_{n \neq 0}^{\infty} (-1)^{(n+1)} \binom{\alpha}{n+1} \\ & \psi(x_l + na) + \frac{t_0}{2} [\psi(x_l - a) + \psi(x_l + a)] - \alpha t_0 \psi(x_l). \quad (7) \end{aligned}$$

Next, we drop the constant diagonal term αt_0 (as it will create only a shift to the energy level). Eqn:(5) becomes,

$$\langle x_l | H | \psi \rangle = \sum_{n \neq 0}^{\infty} t(n) \psi(x_l + na) + \Delta \cos(2\pi\beta l + \phi) \psi(x_l), \quad (8)$$

where $t(n)$ is the hopping parameter for $1 < \alpha \leq 2$,

$$t(n) = \frac{t_0}{2} [(-1)^{|n|+1} \binom{\alpha}{|n|+1} + \delta_{|n|,1}], \quad (9)$$

where $\delta_{n,m}$ is the Kronecker delta.

Now, one can repeat similar calculations for $0 < \alpha < 1$, and gets the following equation,

$$\langle x_l | D_\alpha P^\alpha | \psi \rangle := \frac{t_0}{2} \sum_{n=0}^{\infty} (-1)^n \binom{\alpha}{n} (\psi[x_l + na] + \psi[x_l - na]). \quad (10)$$

Then, $\langle x_l | D_\alpha P^\alpha | \psi \rangle$ becomes⁸⁶,

$$\langle x_l | D_\alpha P^\alpha | \psi \rangle = \frac{t_0}{2} \sum_{n \neq 0}^{\infty} (-1)^n \binom{\alpha}{n} \psi(x_l + na) + t_0 \psi(x_l). \quad (11)$$

Once again, subtracting the constant diagonal terms, one gets,

$$\langle x_l | H | \psi \rangle = \sum_{n \neq 0}^{\infty} t(n) \psi(x_l + na) + \Delta \cos(2\pi\beta l + \phi) \psi(x_l), \quad (12)$$

where $t(n)$, the hopping parameter for $0 < \alpha < 1$ is given by,

$$t(n) = \frac{t_0}{2} [(-1)^{|n|} \binom{\alpha}{|n|}]. \quad (13)$$

Hence in general our model can be written as,

$$H = \sum_{j, n \neq 0} (t(n) c_j^\dagger c_{j+n} + \text{H.c.}) + \Delta \sum_j \cos(2\pi\beta j + \phi) n_j, \quad (14)$$

where, c_j^\dagger (c_j) is the fermionic creation (annihilation) operator at site j , $n_j = c_j^\dagger c_j$ is the number operator,

$$\begin{aligned} t(n) &= -\frac{1}{2} [(-1)^{|n|} \binom{\alpha}{|n|}] & 0 < \alpha < 1, \\ &= \frac{i}{2} \delta_{|n|,1} & \alpha = 1, \\ &= \frac{1}{2} [(-1)^{|n|+1} \binom{\alpha}{|n|+1} + \delta_{|n|,1}] & 1 < \alpha \leq 2. \end{aligned} \quad (15)$$

We do average over ϕ to obtain better statistics and for all of our calculations, we have used periodic boundary conditions.

For $\alpha = 2$, the Hamiltonian H is the same as the Aubry-André (AA) Hamiltonian, which supports a delocalization-localization transition as one tunes Δ . In the thermodynamic limit, $\Delta = 2$ corresponds to the transition point⁶⁶ between localized and delocalized phases and for $\Delta < 2$ ($\Delta > 2$), all the eigenstates of the model are delocalized (localized).

III. ANALYTICAL PREDICTION

Unlike the AA model, the Hamiltonian we are interested in here Eqn. (14), which has higher order hopping terms. It has been shown in Ref.⁸⁷, that in the presence of incommensurate potential with long-range hopping, there exists a mobility edge. One example of such a model is the exponential hopping model (where the hopping amplitudes fall off exponentially with increasing the range n of hopping as $te^{-p|n|}$). This exponential model is self-dual⁸⁷. One can obtain the mobility edge line, using the self-duality condition of the exponential hopping

Hamiltonian, and it is given by the following expression which is taken from Ref.⁸⁷,

$$\cosh(p) = \frac{E + t}{\Delta}. \quad (16)$$

Even though the above expression of ME line is for the self-dual (exponential hopping) model, it has been argued in Ref.⁸⁷ that even the non-dual models (e.g. $t_1 - t_2$ model, Gaussian hopping model, inverse power law hopping model) can be approximated as an exponential model and the analytical mobility edge line (16) gives the qualitatively correct interpretation, if the falling off of the long-range hopping terms is fast enough. However, in general, the energy-dependent mobility edges are not linear in Δ in the case of a non-dual model.

In our case, for the Hamiltonian (14), the long-range hopping terms fall off quickly (see Eqn:(15)). Given the decay is fast enough, that inspires us to approximate the ME line using the expression (16), and we choose $p = \ln \frac{t(1)}{t(2)}$ and $t = t(1)e^{p87}$, where $t(1)$ and $t(2)$ are the nearest neighbor and next nearest neighbor hopping terms, respectively. Next, we will compare our analytic prediction with the numerical results for the finite-size systems.

IV. NUMERICAL RESULTS

Next, we report our numerical findings. One of the most popular diagnostic tools to numerically characterize localized (delocalized) eigenstate is to investigate the Inverse Participation Ratio (IPR). IPR for a normalized eigenstate (k -th) is given by⁶⁸ $\text{IPR}(k) = \sum_{i=1}^L |\psi_i(k)|^4$. For a localized state, IPR approaches its maximum possible value i.e. 1, and for a delocalized state, the IPR value is of the order of $1/L$, which tends to zero in the thermodynamic limit.

Hence, the behavior of the IPR across the mobility edge line is expected to differ, given ME line separates localized and delocalized states in the spectrum. Figure. 2 (upper panel) shows the variation of energy-dependent IPR as a function of $\Delta/t(1)$ for $\alpha = 0.5$. The solid line is the analytic prediction of the ME line obtained from Eqn. (16). Note that even though our analytical prediction is for the self-dual model (exponential hopping Hamiltonian), with an appropriate choice of p , one can see that it gives reasonably well qualitative agreement with our finite-sized numerical results for the Hamiltonian H . However, we can see, as expected here the mobility edge separation is not exactly linear in Δ . Figure. 2(middle panel) shows the variation of the IPR with respect to the energy index k/L . This is a signature of the existence of the ME phase consisting of phases where β^s fraction of states are DL (rest are AL), where $s > 0$ can be any positive integer. We refer to them as p_s ME phases. Next, we also investigate the finite size scaling of participation ratio (PR) for eigenstates. Note that

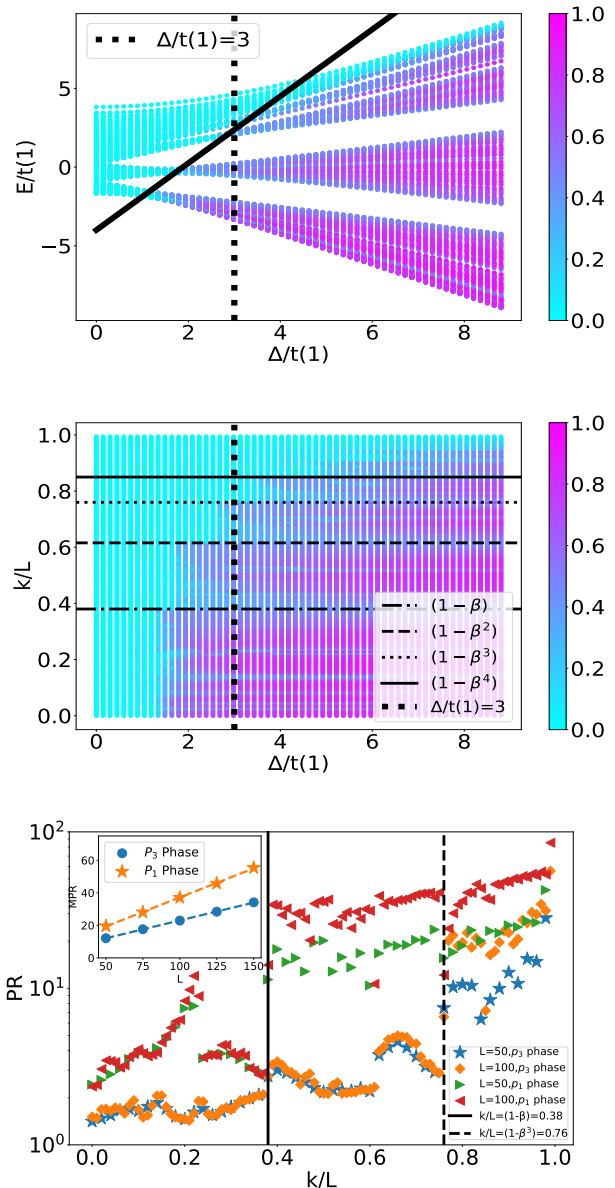


FIG. 2. (Upper panel) Contour plot of Energy dependent IPR vs $\Delta/t(1)$ for the Hamiltonian (14). The solid line shows the analytical separation between delocalized and localized states. (Middle panel) Shows the variation of IPR with respect to energy level index k/L . Results are for $\alpha = 0.5$ and $L = 160$. (Lower panel) Shows the variation of PR with respect to energy level index k/L of p_1 and p_3 phases for different system sizes ($L = 50$ and $L = 100$). Inset shows for both p_1 and p_3 phases, the mean PR value for the delocalized states scales linearly with system size L .

PR is essentially the inverse of IPR, which gives an intuitive measure of localization length. If PR does not scale with system size L , that is a signature of exponentially localized states, where the localization length is independent of system size. On the other hand, PR for delocalized states is expected to increase with L linearly.

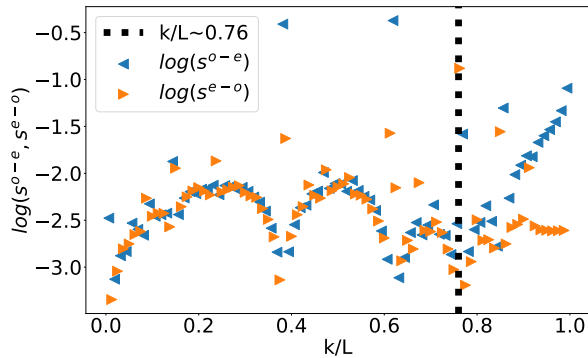


FIG. 3. Shows the variation of level spacing s^{e-o} and s^{o-e} vs k/L . Results are for $\alpha = 0.5$ and $L = 160$.

Figure 2 (lower panel) confirms that for both for p_1 and p_3 phases indeed β and β^3 fraction of states are delocalized. Moreover, the inset shows that the mean PR for the delocalized states scales linearly with L , which excludes the possibility of having multifractal states. (Note, the scaling of the participation ratio is sub-linear in L for the multifractal phase⁸⁸.)

We also strengthen our finding from the even-odd and odd-even level spacing statistics⁸⁸. Even-Odd and odd-Even spacing are given by, $s_k^{e-o} = E_{2k} - E_{2k-1}$, $s_k^{o-e} = E_{2k+1} - E_{2k}$, where E_k s are the energy eigenvalues of the single-particle spectrum arranged in ascending order. For the delocalized single-particle states, there exist almost doubly degenerate spectra^{66,88}, so there is a gap between s_k^{e-o} and s_k^{o-e} . On the other hand, for the localized single-particle states, that degeneracy is lifted, hence the gap between s_k^{e-o} and s_k^{o-e} vanishes. Figure 3 clearly demonstrates that. We choose $\Delta/t(1) = 3$ [which denoted by dashed line in Fig. 2 (upper panel)]. It is clear from Fig. 2 (upper panel), for this choice of parameter, the single-particle spectrum has a ME (which corresponds to $k/L = 0.76 \simeq 1 - \beta^3$; p_3 ME phase). Figure 3 shows clearly that s^{e-o} and s^{o-e} fall on top of each other for $k/L < 0.76$ and for $k/L > 0.76$ there is a gap, which indicates the existence of the localized and delocalized phase respectively. We identify this point with a black circle in Fig. 1. Also, it is important to point out that in the multifractal phase, s^{e-o} and s^{o-e} both are strongly scattered, we don't see any evidence of that in our results. Results for $\alpha = 1.5$ are shown in Fig: 6. We repeat our analysis for different values of α and obtain the complete phase diagram which is shown in Fig. 1 (see Appendix:C for details).

V. EFFECTIVE HAMILTONIAN

From our numerical study it is obvious that the phase diagram for Lévy quasicrystal is very similar to the long-range hopping model studied in Ref.⁸⁸. We study the

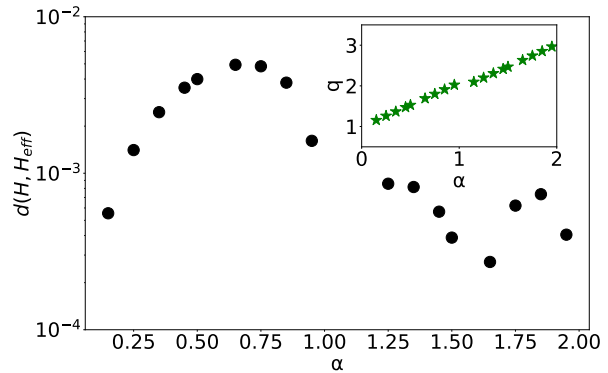
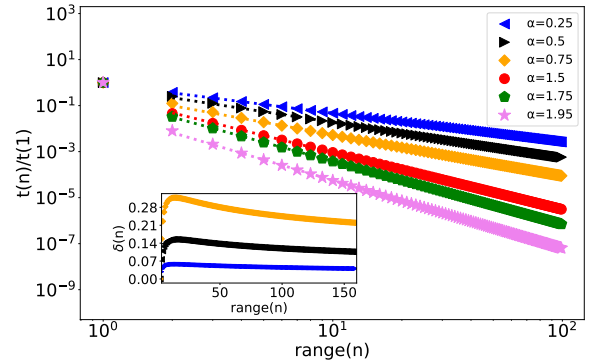


FIG. 4. Upper panel: Variation of $t(n)/t(1)$ vs range n for $L = 100$ for different values of α . Dashed lines show the power-law fit for $n \geq 2$. Inset shows the variation of the difference between the hopping terms coming from the Hamiltonian (14) and H_{eff} normalized by the hopping terms coming from the Hamiltonian (14) (denoted by δ) with range n . Lower panel: The normalized trace distance between H and H_{eff} as a function of α . The inset shows the variation q with α .

variation of $t(n)/t(1)$ vs n in the upper panel of Fig. 4. We find that the fall-off of hopping amplitude for the range $n \geq 2$, $t(n) \sim t(2)/|n/2|^q$, where q depends on α . Hence, we write down an effective Hamiltonian,

$$H_{eff} = \sum_j t(1)(c_j^\dagger c_{j+1} + \text{H.c.}) + \sum_{j,n>1} \frac{t(2)}{|n/2|^q} (c_j^\dagger c_{j+n} + \text{H.c.}) + \Delta \sum_j \cos(2\pi\beta j + \phi) n_j, \quad (17)$$

and compare it with Lévy quasicrystal. In the large n limit, it can be shown analytically that $q \simeq \alpha + 1$ (see Appendix: D), and the q obtained from the numerical calculations (see inset of the lower panel of Fig. 4) also show a similar result. The structure of this effective Hamiltonian is quite similar to the previously studied AA models with power-law hopping in Ref.^{88,89} except that in our case we have an extra nearest-neighbor hopping term. We like to emphasize that while Fig. 4 (upper panel) might suggest that H_{eff} is an extremely accurate

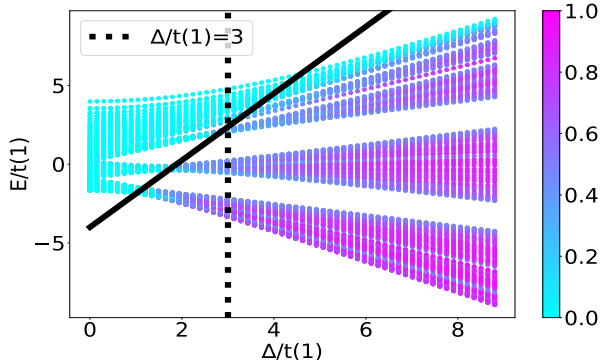
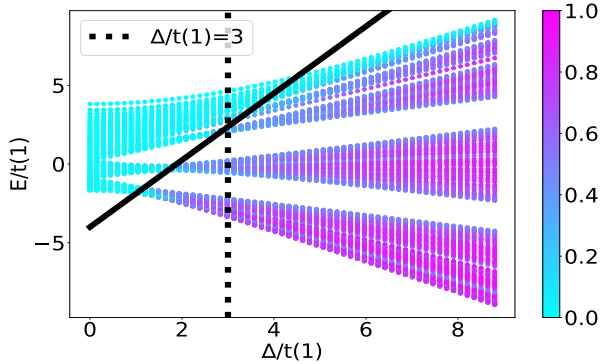


FIG. 5. (Upper panel) Contour plot of Energy dependent IPR vs $\Delta/t(1)$ for the Hamiltonian H . Solid lines show analytical separation between delocalized and localized states. (Lower panel) Contour plot of Energy dependent IPR vs $\Delta/t(1)$ for the Hamiltonian H_{eff} for $q = 1.528$. Solid lines show analytical separation between delocalized and localized states. Results are for $\alpha = 0.5$ and $L = 160$.

description of the Lévy quasicrystal, a careful study suggests that there are significant differences. In the inset, we show the variation of the relative difference in hopping amplitudes between these two models, which is defined as

$$\delta(n) = \frac{|t^H(n) - t^{H_{\text{eff}}}(n)|}{t^H(n)}, \quad (18)$$

where t^H and $t^{H_{\text{eff}}}$ stands for hopping amplitudes of Lévy quasicrystal and effective power-law hopping Hamiltonian respectively. The relative difference is more than 20% for some values of α (see inset of Fig. 4 upper panel). Moreover, we also calculate the normalized trace distance⁹⁰ between the Hamiltonian H (14) and H_{eff} . The normalized trace distance is defined as follows, $d(H, H_{\text{eff}}) = \frac{1}{L} \text{Tr}[\sqrt{(H - H_{\text{eff}})^2}]$. Lower panel of Figure. 4 shows the variation of $d(H, H_{\text{eff}})$ with α , this trace difference between two Hamiltonians are small $< 10^{-2}$, but not negligible. Hence, one can conclude that H_{eff} is a reasonably good approximation of our original Hamiltonian H , but they still have significant differences.

Hence, it is not obvious that both of these Hamiltoni-

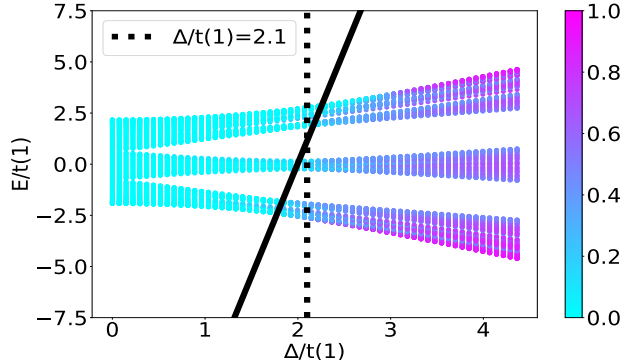
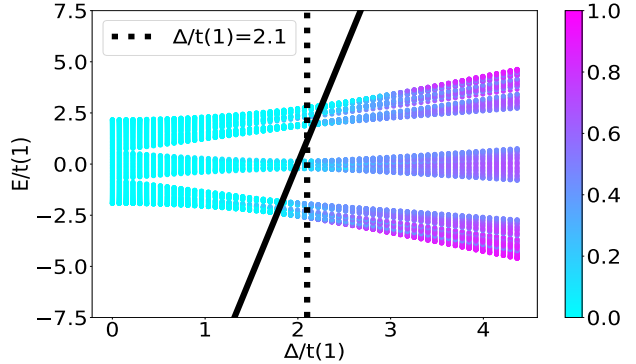


FIG. 6. (Upper panel) Contour plot of Energy dependent IPR vs $\Delta/t(1)$ for the Hamiltonian H . Solid lines show analytical separation between delocalized and localized states. (Lower panel) Contour plot of Energy dependent IPR vs $\Delta/t(1)$ for the Hamiltonian H_{eff} for $q = 2.4689$. Solid lines show analytical separation between delocalized and localized states. Results are for $\alpha = 1.5$ and $L = 160$.

ans will show a similar phase diagram. Next, we compare the energy-dependent IPR for both the Hamiltonians (H and H_{eff}) and remarkably find that they are almost qualitatively very similar. We show the results for $\alpha = 0.5$ and 1.5 and compare them with H_{eff} results. The results of the energy-dependent IPR are shown in Fig. 5 and Fig. 6 respectively. The solid line represents the ME line obtained using Eqn. 16. It seems that the analytic prediction of the ME line does qualitatively a very good job for $\alpha = 1.5$ compared to $\alpha = 0.5$, presumably because $t(2)/t(1)$ is much smaller for $\alpha = 1.5$. It's in great agreement with our numerical prediction. This gives us the validation that indeed H_{eff} is a good approximation to our original Hamiltonian H even though they are not identical (see Appendix. B).

Also, this effective Hamiltonian can be experimentally probed for polar molecules pinned in deep bichromatic optical lattices. Powers $1 \leq q \leq 3$ (which is also what we have obtained for our model) may be directly realized in ions^{91,92}.

VI. CONCLUSIONS

In this work, we define Lévy quasicrystal by discretizing the space-fractional Schrödinger equation using the Grünwald derivatives and adding on-site quasiperiodic potential and investigate the phase diagram. We find that while there exists a parameter region where all states are either completely delocalized or completely localized as one will observe for normal quasicrystal, there also exists a region where delocalized and localized states coexist and are separated by a mobility edge. Moreover, based on the fraction of DL states, we identify different p_s ME phases. Similar phases have been observed in the AA model with power-law hopping^{88,89}. Hence, we compare our results with the effective power-law hopping model as well. To the best of our knowledge such p_s ME phases have not been observed in any other models so far except for the power-law hopping models. Our results prove that similar p_s phases can be found even for models where the fall-off of hopping amplitudes are not strictly power-law type. It opens up a broader question, in order to have p_s ME phases, what necessary condition one needs to impose on hopping amplitude? Our study also shows a connection between p_s ME phases with SFQM, which might be an important step forward in understanding the origins of such p_s ME phases. It is well established that to understand the traveling behavior of animals^{14,15}, the complex dynamics of real-life financial markets¹⁸, Lévy description has been extremely useful. If one wants to model a situation to understand how these things can get affected due to correlated random events, our Lévy quasicrystal will be an automatic choice. One of the biggest advantages of Lévy quasicrystal is that apart from the localized and delocalized phases; it also supports a mixed phase (mobility edges that separate localized and delocalized states). This can be thought of as those random correlated events that affect the motions of some animals while the motions of other animals are unaffected. On top of that, the existence of different p_s mobility edge phases (which is unique for our model) gives us extreme control over the ratio of the number of animals whose motion gets restricted (localized states) and the number of animals that can still move freely (delocalized states). Note that one can get all this control in our model with only two free parameters, i.e., α (Lévy index) and Δ (strength of correlated random potential).

Moreover, in the optical system, there has been a proposal to experimentally realize a very similar model²⁶, we strongly believe our study should motivate experimentalists to revisit the same model and identify such p_s mobility edge phases. We also think that given there are similarities in the phase diagram between Lévy quasicrystal and power-law hopping models, it makes Lévy quasicrystal a probable candidate for the experimentally accessible realization of space-fractional quantum mechanics (SFQM) in a condensed-matter set-up. Further, it will be interesting to investigate the role of interaction⁹³⁻⁹⁵ and the effect of the Hermiticity breaking and the PT

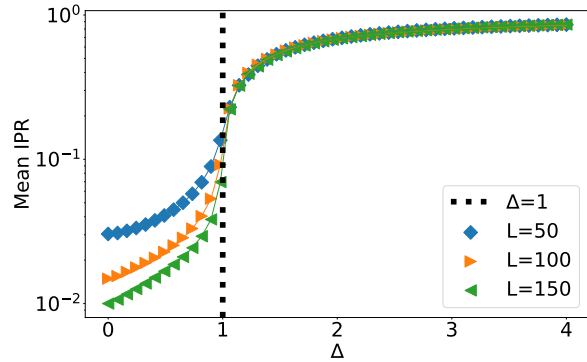


FIG. 7. Variation of Mean IPR vs Δ for the $\alpha = 1$ model Eqn. A2. The vertical dashed line shows the transition i.e. $\Delta = 1$.

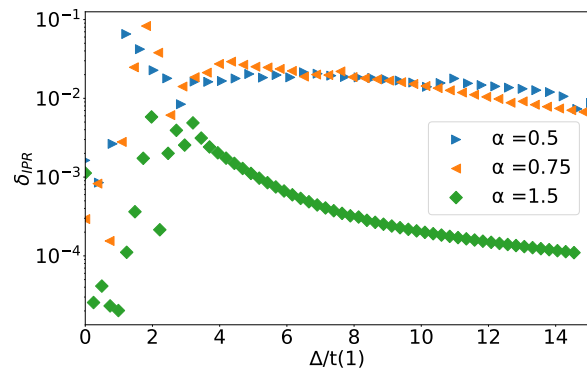


FIG. 8. Variation of relative difference of mean IPR between H and H_{eff} vs $\Delta/t(1)$ for different values of α .

symmetry⁹⁶⁻⁹⁸ in the context of SFQM.

VII. ACKNOWLEDGEMENTS

RM acknowledges the DST-Inspire research grant by the Department of Science and Technology, Government of India, SERB start-up grant (SRG/2021/002152). The authors thank Vikash Pandey and Bhabani Prasad Mandal for introducing the topic of Space-fractional quantum mechanics. Authors also thank Sambuddha Sanyal for fruitful discussions.

Appendix A: $\alpha = 1$ Model

In the main text, we introduce Lévy quasicrystal by discretizing the space-fractional Schrödinger equation using the Grünwald-Letnikov derivatives and adding on-site quasiperiodic potential. However, this discretization technique works for $\alpha \in (0, 2]$ except $\alpha = 1$. Hence, we focus on the $\alpha = 1$ model separately.

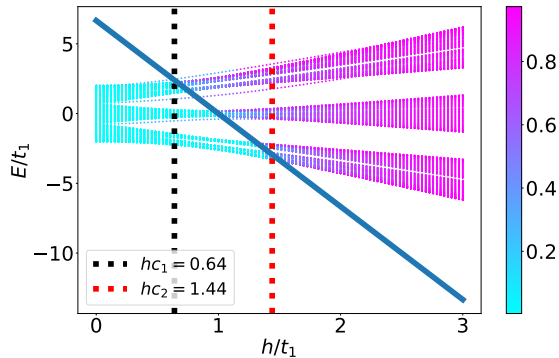


FIG. 9. Contour plot of energy dependent IPR vs $\frac{h}{t_1}$ for the GAA hamiltonian(C1). The solid blue line shows the exact separation of delocalized and localized states, given by Eqn.(C2). Dashed black and red lines show the transition points calculated from the tolerance method. Here we take $\gamma = 0.3$ and $t_1 = 1$

For $\alpha = 1$, $\langle x_l | D_\alpha P^\alpha | \psi \rangle$ becomes,

$$\langle x_l | D_\alpha P^\alpha | \psi \rangle = \frac{i}{2a} [\psi(x_l + a) - \psi(x_l - a)], \quad (\text{A1})$$

where a is the lattice constant. The Hamiltonian H is given by,

$$H = \sum_j \frac{1}{2} (i c_j^\dagger c_{j+1} + \text{H.c.}) + \Delta \sum_j \cos(2\pi\beta j + \phi) n_j. \quad (\text{A2})$$

Note that for $\Delta = 0$, the energy dispersion relation of the Hamiltonian is $E(k) = \sin k$, in the continuum limit i.e. $k \rightarrow 0$, $E(k) \sim k$ (linear dispersion model). This model shows localization-delocalization transition at $\Delta = 1$. We have shown this by calculating Mean IPR as a function of Δ in Fig. 7.

Appendix B: Comparison between Mean IPR of H and H_{eff}

In the main text, we have shown results for energy-dependent IPR for Lévy quasicrystal and H_{eff} . While these two models are not identical but the IPR results look qualitatively very similar (see Fig. 5 and Fig. 6). We define the relative difference of mean IPR (M) between H and H_{eff} as,

$$\delta_{IPR} = \frac{|M_H - M_{H_{eff}}|}{M_H}. \quad (\text{B1})$$

Figure. 8 shows the variation δ_{IPR} vs $\Delta/t(1)$ for different values of α , and we find that the relative difference is less than 10%. Note that on the other hand, the relative difference in hopping amplitude between these two models is almost 20% as discussed in the main text.

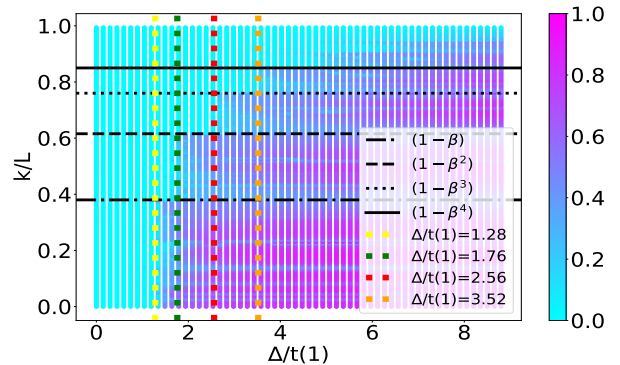


FIG. 10. Shows the variation of IPR with respect to energy level index k/L . for $\alpha = 0.5$. Vertical lines are phase boundaries between different p_s phases obtained from the tolerance criteria.

Appendix C: Method for detecting different phases for finite system

While IPR is an extremely useful diagnostic to detect localized and delocalized states, in order to really identify DL and AL states, one needs to do a finite-size scaling analysis. Given our Hamiltonian H involves terms having Gamma function in the hopping parameter, numerically it is very difficult to study large systems, especially beyond $L = 200$ (long-range hopping terms can't be calculated accurately). Hence, in this work, we are restricted to small system sizes, and doing a proper finite size analysis is tricky. In order to understand the delocalization-localization transition, we use tolerance criteria based on the finite-size AA model. We calculate the difference between mean PR for the AA model (for the Hamiltonian H i.e. $\alpha = 2$ and $\Delta = 2$) for two system sizes L_1 and L_2 at the transition point i.e. $\epsilon = PR(L_1) - PR(L_2)$. We use that value to detect different phases.

First, we use this criteria for the Generalized Aubry-André model, which is given by,⁹⁴

$$\tilde{H} = \sum_j t_1 (c_j^\dagger c_{j+1} + \text{H.c.}) + 2h \sum_j \frac{\cos(2\pi\beta j + \phi)}{1 - \gamma \cos(2\pi\beta j + \phi)} n_j. \quad (\text{C1})$$

where $\gamma \in (-1, 1)$. This model is having an exact analytical solution for the mobility edge line as,

$$\gamma E = 2 \text{sgn}(h) (|t_1| - |h|). \quad (\text{C2})$$

We use our tolerance criteria on the ground state and the highest excited state for the same L_1 and L_2 for which the tolerance criteria for the AA model have been obtained, to identify hc_1 (below which all states are DL) and hc_2 (above which all states are AL). They are in great agreement with the exact analytical ME prediction as shown in Fig. (9).

That motivates us to go forward and use the same criteria to detect different p_s ME phases in the H . We calculate PR for the Hamiltonian H for m th eigenstate (m is the nearest integer of $(1 - \beta^s)L - 1$) for different values of Δ , whenever they match with our tolerance criteria, we identify that value of Δ as a transition point between p_{s-1} ME phase to p_s ME phase (p_0 phase can be thought of DL phase). Figure. 10 clearly demonstrate that our criteria do a reasonably good job of identifying those phases. We use this technique to obtain the phase diagram which is presented in the main text. We have repeated our calculation for large systems for H_{eff} and obtained a very similar phase diagram as well.

Appendix D: Analytical prediction: the equivalence between H and H_{eff} in large n limit

Using the reflection property of Gamma function one can write,

$$\Gamma(z)\Gamma(1-z) = \frac{\pi}{\sin(z\pi)}$$

Moreover,

$$\Gamma(|n| - \alpha)\Gamma(1 - |n| + \alpha) = \frac{\pi}{\sin[(|n| - \alpha)\pi]} = \frac{\pi(-1)^{(|n|-1)}}{\sin(\pi\alpha)}$$

Now, $\sin(\alpha\pi) = \frac{\pi}{\Gamma(-1-\alpha)\Gamma(2+\alpha)}$, substituting this value to the above equation we can write

$$\Gamma(1 - |n| + \alpha) = \frac{(-1)^{|n|-1}\Gamma(-1 - \alpha)\Gamma(\alpha + 2)}{\Gamma(|n| - \alpha)} \quad (\text{D1})$$

Now for $0 < \alpha < 1$ limit,

$$\begin{aligned} t(n) &= -\frac{1}{2}[(-1)^{|n|}\binom{\alpha}{|n|}] \\ &= -\frac{1}{2}\frac{(-1)^{|n|}\Gamma(\alpha+1)}{\Gamma(|n|+1)\Gamma(\alpha-|n|+1)} \end{aligned}$$

Now taking $n \rightarrow \infty$ limit and using Stirling's formula ($\Gamma(|n| - \alpha) \approx \sqrt{2\pi}(|n| - \alpha)^{(|n| - \alpha) - \frac{1}{2}} e^{-(|n| - \alpha)}$ and

$\Gamma(|n| + 1) \approx \sqrt{2\pi}(|n| + 1)^{(|n| + 1) - \frac{1}{2}} e^{-(|n| + 1)}$), and using Eqn:(D1), $t(n)$ becomes,

$$t(n) \simeq \frac{1}{2} \frac{e^{\alpha-1}}{(\alpha+1)\Gamma(-1-\alpha)} \frac{1}{|n|^{\alpha+1}}, \quad \text{for } 0 < \alpha < 1 \quad (\text{D2})$$

Similarly using the reflection property of the Gamma function one can write,

$$\begin{aligned} \Gamma(\alpha - |n|) &= \frac{-(-1)^{|n|-1}\pi}{\Gamma(|n| - \alpha + 1)\sin(\alpha\pi)} \\ \text{or, } \Gamma(\alpha - |n|) &= \frac{-(-1)^{|n|-1}\Gamma(-1 - \alpha)\Gamma(\alpha + 2)}{\Gamma(|n| - \alpha + 1)} \quad (\text{D3}) \end{aligned}$$

For the limit $1 < \alpha < 2$,

$$\begin{aligned} t(n) &= \frac{1}{2}[(-1)^{|n|+1}\binom{\alpha}{|n|+1}] \\ &= \frac{1}{2}\frac{(-1)^{|n|+1}\Gamma(\alpha+1)}{\Gamma(|n|+2)\Gamma(\alpha-|n|)} \end{aligned}$$

Taking $n \rightarrow \infty$ limit and using Stirling's formula ($\Gamma(|n| - \alpha + 1) \approx \sqrt{2\pi}(|n| - \alpha + 1)^{(|n| - \alpha + 1) - \frac{1}{2}} e^{-(|n| - \alpha + 1)}$ and $\Gamma(|n| + 2) \approx \sqrt{2\pi}(|n| + 2)^{(|n| + 2) - \frac{1}{2}} e^{-(|n| + 2)}$), and using Eqn:(D3), $t(n)$ becomes,

$$t(n) \simeq -\frac{1}{2} \frac{e^{\alpha+1}}{(\alpha+1)\Gamma(-1-\alpha)} \frac{1}{|n|^{\alpha+1}}, \quad \text{for } 1 < \alpha < 2 \quad (\text{D4})$$

Hence, indeed in the large n limit, the hopping parameter $t(n)$ shows power law behavior.

* ph22d001@iittp.ac.in

† ranjan@iittp.ac.in

- 1 C.A. Dartora, Fernando Zanella, and G.G. Cabrera, "Emergence of fractional quantum mechanics in condensed matter physics," *Physics Letters A* **415**, 127643 (2021).
- 2 Nikolai Laskin, "Fractional quantum mechanics and lévy path integrals," *Physics Letters A* **268**, 298–305 (2000).
- 3 Nick Laskin, "Fractional quantum mechanics," *Phys. Rev. E* **62**, 3135–3145 (2000).
- 4 Nick Laskin, "Fractional schrödinger equation," *Phys. Rev. E* **66**, 056108 (2002).
- 5 B. A. Stickler, "Potential condensed-matter realization of space-fractional quantum mechanics: The one-dimensional lévy crystal," *Phys. Rev. E* **88**, 012120 (2013).
- 6 Mohammad Hasan and Bhabani Prasad Mandal, "Tunneling time in space fractional quantum mechanics," *Physics Letters A* **382**, 248–252 (2018).
- 7 Yiqi Zhang, Xing Liu, Milivoj R. Belić, Weiping Zhong, Yanpeng Zhang, and Min Xiao, "Propagation dynamics of a light beam in a fractional schrödinger equation," *Phys.*

Rev. Lett. **115**, 180403 (2015).

- 8 Christian B Mendl and Herbert Spohn, "Current fluctuations for anharmonic chains in thermal equilibrium," *Journal of Statistical Mechanics: Theory and Experiment* **2015**, P03007 (2015).
- 9 Henk van Beijeren, "Exact results for anomalous transport in one-dimensional hamiltonian systems," *Phys. Rev. Lett.* **108**, 180601 (2012).
- 10 Abhishek Dhar, Keiji Saito, and Bernard Derrida, "Exact solution of a lévy walk model for anomalous heat transport," *Physical Review E* **87**, 010103 (2013).
- 11 Aritra Kundu, Cédric Bernardin, Keji Saito, Anupam Kundu, and Abhishek Dhar, "Fractional equation description of an open anomalous heat conduction set-up," *Journal of Statistical Mechanics: Theory and Experiment* **2019**, 013205 (2019).
- 12 T. H. Solomon, Eric R. Weeks, and Harry L. Swinney, "Observation of anomalous diffusion and lévy flights in a two-dimensional rotating flow," *Phys. Rev. Lett.* **71**, 3975–3978 (1993).

- ¹³ Vikash Pandey and Sverre Holm, “Linking the fractional derivative and the lomnitz creep law to non-newtonian time-varying viscosity,” *Phys. Rev. E* **94**, 032606 (2016).
- ¹⁴ Dirk Brockmann, Lars Hufnagel, and Theo Geisel, “The scaling laws of human travel,” *Nature* **439**, 462–465 (2006).
- ¹⁵ Simon Benhamou, “How many animals really do the lévy walk?” *Ecology* **88**, 1962–1969 (2007).
- ¹⁶ Yuxi Liu, Xian Long, Paul R Martin, Samuel G Solomon, and Pulin Gong, “Lévy walk dynamics explain gamma burst patterns in primate cerebral cortex,” *Communications Biology* **4**, 739 (2021).
- ¹⁷ Hisashi Murakami, Claudio Feliciani, and Katsuhiko Nishinari, “Lévy walk process in self-organization of pedestrian crowds,” *Journal of The Royal Society Interface* **16**, 20180939 (2019).
- ¹⁸ Hediye Yarahmadi and Abbas Ali Saberi, “A 2d lévy-flight model for the complex dynamics of real-life financial markets,” *Chaos: An Interdisciplinary Journal of Nonlinear Science* **32**, 033113 (2022).
- ¹⁹ Adam M Kaufman, M Eric Tai, Alexander Lukin, Matthew Rispoli, Robert Schittko, Philipp M Preiss, and Markus Greiner, “Quantum thermalization through entanglement in an isolated many-body system,” *Science* **353**, 794–800 (2016).
- ²⁰ Dmitry A. Abanin, Ehud Altman, Immanuel Bloch, and Maksym Serbyn, “Colloquium: Many-body localization, thermalization, and entanglement,” *Rev. Mod. Phys.* **91**, 021001 (2019).
- ²¹ Michael Schreiber, Sean S Hodgman, Pranjali Bordia, Henrik P Lüschen, Mark H Fischer, Ronen Vosk, Ehud Altman, Ulrich Schneider, and Immanuel Bloch, “Observation of many-body localization of interacting fermions in a quasirandom optical lattice,” *Science* **349**, 842–845 (2015).
- ²² Alexander Iomin, “Fractional schrödinger equation in gravitational optics,” *Modern Physics Letters A* **36**, 2140003 (2021).
- ²³ Liangwei Zeng and Jianhua Zeng, “One-dimensional solitons in fractional schrödinger equation with a spatially periodical modulated nonlinearity: nonlinear lattice,” *Optics Letters* **44**, 2661–2664 (2019).
- ²⁴ Wang Xin, Lijun Song, and Lu Li, “Propagation of gaussian beam based on two-dimensional fractional schrödinger equation,” *Optics Communications* **480**, 126483 (2021).
- ²⁵ Shangling He, Boris A Malomed, Dumitru Mihalache, Xi Peng, Yingji He, and Dongmei Deng, “Propagation dynamics of radially polarized symmetric airy beams in the fractional schrödinger equation,” *Physics Letters A* **404**, 127403 (2021).
- ²⁶ Changming Huang, Ce Shang, Jing Li, Liangwei Dong, and Fangwei Ye, “Localization and anderson delocalization of light in fractional dimensions with a quasi-periodic lattice,” *Optics Express* **27**, 6259–6267 (2019).
- ²⁷ Yiqi Zhang, Xing Liu, Milivoj R. Belić, Weiping Zhong, Yanpeng Zhang, and Min Xiao, “Propagation dynamics of a light beam in a fractional schrödinger equation,” *Phys. Rev. Lett.* **115**, 180403 (2015).
- ²⁸ Shatrughna Kumar, Pengfei Li, and Boris A Malomed, “Domain walls in fractional media,” *Physical Review E* **106**, 054207 (2022).
- ²⁹ Pengfei Li, Jiandan Li, Bingchen Han, Huifang Ma, and Dumitru Mihalache, “Pt-symmetric optical modes and spontaneous symmetry breaking in the space-fractional schrödinger equation,” *Rom. Rep. Phys* **71**, 106 (2019).
- ³⁰ Liangwei Zeng, Jincheng Shi, Xiaowei Lu, Yi Cai, Qifan Zhu, Hongyi Chen, Hu Long, and Jingzhen Li, “Stable and oscillating solitons of pt-symmetric couplers with gain and loss in fractional dimension,” *Nonlinear Dynamics* **103**, 1831–1840 (2021).
- ³¹ Pengfei Li, Boris A Malomed, and Dumitru Mihalache, “Symmetry-breaking bifurcations and ghost states in the fractional nonlinear schrödinger equation with a pt-symmetric potential,” *Optics Letters* **46**, 3267–3270 (2021).
- ³² Boris A Malomed, “Optical solitons and vortices in fractional media: A mini-review of recent results,” in *Photonics*, Vol. 8 (Mdpi, 2021) p. 353.
- ³³ Yunli Qiu, Boris A Malomed, Dumitru Mihalache, Xing Zhu, Li Zhang, and Yingji He, “Soliton dynamics in a fractional complex ginzburg-landau model,” *Chaos, Solitons & Fractals* **131**, 109471 (2020).
- ³⁴ Liangwei Zeng, Yongle Zhu, Boris A Malomed, Dumitru Mihalache, Qing Wang, Hu Long, Yi Cai, Xiaowei Lu, and Jingzhen Li, “Quadratic fractional solitons,” *Chaos, Solitons & Fractals* **154**, 111586 (2022).
- ³⁵ Liangwei Zeng and Jianhua Zeng, “Fractional quantum couplers,” *Chaos, Solitons & Fractals* **140**, 110271 (2020).
- ³⁶ Pengfei Li, Rujiang Li, and Chaoqing Dai, “Existence, symmetry breaking bifurcation and stability of two-dimensional optical solitons supported by fractional diffraction,” *Optics Express* **29**, 3193–3210 (2021).
- ³⁷ Pengfei Li, Boris A Malomed, and Dumitru Mihalache, “Symmetry breaking of spatial kerr solitons in fractional dimension,” *Chaos, Solitons & Fractals* **132**, 109602 (2020).
- ³⁸ Pengfei Li and Chaoqing Dai, “Double loops and pitchfork symmetry breaking bifurcations of optical solitons in nonlinear fractional schrödinger equation with competing cubic-quintic nonlinearities,” *Annalen der Physik* **532**, 2000048 (2020).
- ³⁹ Liangwei Zeng, Boris A Malomed, Dumitru Mihalache, Yi Cai, Xiaowei Lu, Qifan Zhu, and Jingzhen Li, “Bubbles and w-shaped solitons in kerr media with fractional diffraction,” *Nonlinear Dynamics* **104**, 4253–4264 (2021).
- ⁴⁰ Mario I Molina, “The two-dimensional fractional discrete nonlinear schrödinger equation,” *Physics Letters A* **384**, 126835 (2020).
- ⁴¹ Liangwei Zeng and Jianhua Zeng, “Preventing critical collapse of higher-order solitons by tailoring unconventional optical diffraction and nonlinearities,” *Communications Physics* **3**, 26 (2020).
- ⁴² Liangwei Zeng, Dumitru Mihalache, Boris A Malomed, Xiaowei Lu, Yi Cai, Qifan Zhu, and Jingzhen Li, “Families of fundamental and multipole solitons in a cubic-quintic nonlinear lattice in fractional dimension,” *Chaos, Solitons & Fractals* **144**, 110589 (2021).
- ⁴³ Pengfei Li, Boris A Malomed, and Dumitru Mihalache, “Metastable soliton necklaces supported by fractional diffraction and competing nonlinearities,” *Optics Express* **28**, 34472–34488 (2020).
- ⁴⁴ Yunli Qiu, Boris A Malomed, Dumitru Mihalache, Xing Zhu, Xi Peng, and Yingji He, “Stabilization of single- and multi-peak solitons in the fractional nonlinear schrödinger equation with a trapping potential,” *Chaos, Solitons & Fractals* **140**, 110222 (2020).
- ⁴⁵ Liangwei Zeng and Jianhua Zeng, “One-dimensional solitons in fractional schrödinger equation with a spatially periodical modulated nonlinearity: nonlinear lattice,” *Optics Letters* **44**, 2661–2664 (2019).

- ⁴⁶ Qing Wang and Guo Liang, “Vortex and cluster solitons in nonlocal nonlinear fractional schrödinger equation,” *Journal of Optics* **22**, 055501 (2020).
- ⁴⁷ Pengfei Li, Boris A Malomed, and Dumitru Mihalache, “Vortex solitons in fractional nonlinear schrödinger equation with the cubic-quintic nonlinearity,” *Chaos, Solitons & Fractals* **137**, 109783 (2020).
- ⁴⁸ Liangwei Zeng and Jianhua Zeng, “One-dimensional gap solitons in quintic and cubic–quintic fractional nonlinear schrödinger equations with a periodically modulated linear potential,” *Nonlinear Dynamics* **98**, 985–995 (2019).
- ⁴⁹ Liangwei Dong and Zhaoxia Tian, “Truncated-bloch-wave solitons in nonlinear fractional periodic systems,” *Annals of Physics* **404**, 57–65 (2019).
- ⁵⁰ Lifu Zhang, Xiang Zhang, Haozhe Wu, Chuxin Li, Davide Pierangeli, Yanxia Gao, and Dianyuan Fan, “Anomalous interaction of airy beams in the fractional nonlinear schrödinger equation,” *Opt. Express* **27**, 27936–27945 (2019).
- ⁵¹ Jing Xiao, Zhaoxia Tian, Changming Huang, and Liangwei Dong, “Surface gap solitons in a nonlinear fractional schrödinger equation,” *Optics Express* **26**, 2650–2658 (2018).
- ⁵² Qing Wang and ZhenZhou Deng, “Elliptic solitons in (1+2)-dimensional anisotropic nonlocal nonlinear fractional schrödinger equation,” *IEEE Photonics Journal* **11**, 1–8 (2019).
- ⁵³ Qing Wang, Jingzhen Li, Lifu Zhang, and Weixin Xie, “Hermite-gaussian-like soliton in the nonlocal nonlinear fractional schrödinger equation,” *Europhysics Letters* **122**, 64001 (2018).
- ⁵⁴ Manna Chen, Shihao Zeng, Daquan Lu, Wei Hu, and Qi Guo, “Optical solitons, self-focusing, and wave collapse in a space-fractional schrödinger equation with a kerr-type nonlinearity,” *Physical Review E* **98**, 022211 (2018).
- ⁵⁵ Shilong Liu, Yingwen Zhang, Boris A Malomed, and Ebrahim Karimi, “Experimental realisations of the fractional schrödinger equation in the temporal domain,” *Nature Communications* **14**, 222 (2023).
- ⁵⁶ Gadi Afek, Nir Davidson, David A Kessler, and Eli Barkai, “Anomalous statistics of laser-cooled atoms in dissipative optical lattices,” *arXiv preprint arXiv:2107.09526* (2021).
- ⁵⁷ S. Marksteiner, K. Ellinger, and P. Zoller, “Anomalous diffusion and lévy walks in optical lattices,” *Phys. Rev. A* **53**, 3409–3430 (1996).
- ⁵⁸ Elihu Abrahams, PW Anderson, DC Licciardello, and TV Ramakrishnan, “Scaling theory of localization: Absence of quantum diffusion in two dimensions,” *Physical Review Letters* **42**, 673–676 (1979).
- ⁵⁹ Patrick A Lee and TV Ramakrishnan, “Disordered electronic systems,” *Reviews of Modern Physics* **57**, 287 (1985).
- ⁶⁰ Philip W Anderson, “Absence of diffusion in certain random lattices,” *Physical review* **109**, 1492 (1958).
- ⁶¹ Jens H. Bardarson, Frank Pollmann, and Joel E. Moore, “Unbounded growth of entanglement in models of many-body localization,” *Phys. Rev. Lett.* **109**, 017202 (2012).
- ⁶² Ronen Vosk and Ehud Altman, “Many-body localization in one dimension as a dynamical renormalization group fixed point,” *Phys. Rev. Lett.* **110**, 067204 (2013).
- ⁶³ Denis M Basko, Igor L Aleiner, and Boris L Altshuler, “Metal–insulator transition in a weakly interacting many-electron system with localized single-particle states,” *Annals of physics* **321**, 1126–1205 (2006).
- ⁶⁴ Soumi Ghosh, Atithi Acharya, Subhayan Sahu, and Subroto Mukerjee, “Many-body localization due to correlated disorder in fock space,” *Phys. Rev. B* **99**, 165131 (2019).
- ⁶⁵ Jagannath Sutradhar, Soumi Ghosh, Sthitadhi Roy, David E. Logan, Subroto Mukerjee, and Sumilan Banerjee, “Scaling of the fock-space propagator and multifractality across the many-body localization transition,” *Phys. Rev. B* **106**, 054203 (2022).
- ⁶⁶ Serge Aubry and Gilles André, “Analyticity breaking and anderson localization in incommensurate lattices,” *Ann. Israel Phys. Soc* **3**, 18 (1980).
- ⁶⁷ J. T. Chayes, L. Chayes, Daniel S. Fisher, and T. Spencer, “Finite-size scaling and correlation lengths for disordered systems,” *Phys. Rev. Lett.* **57**, 2999–3002 (1986).
- ⁶⁸ Dong-Ling Deng, Sriram Ganeshan, Xiaopeng Li, Ranjan Modak, Subroto Mukerjee, and JH Pixley, “Many-body localization in incommensurate models with a mobility edge,” *Annalen der Physik* **529**, 1600399 (2017).
- ⁶⁹ Xiao Li and S. Das Sarma, “Mobility edge and intermediate phase in one-dimensional incommensurate lattice potentials,” *Phys. Rev. B* **101**, 064203 (2020).
- ⁷⁰ Sriram Ganeshan, J. H. Pixley, and S. Das Sarma, “Nearest neighbor tight binding models with an exact mobility edge in one dimension,” *Phys. Rev. Lett.* **114**, 146601 (2015).
- ⁷¹ Fangzhao Alex An, Karmela Padavić, Eric J. Meier, Suraj Hegde, Sriram Ganeshan, J. H. Pixley, Smitha Vishveshwara, and Bryce Gadway, “Interactions and mobility edges: Observing the generalized aubry-andré model,” *Phys. Rev. Lett.* **126**, 040603 (2021).
- ⁷² Dave J. Boers, Benjamin Goedeke, Dennis Hinrichs, and Martin Holthaus, “Mobility edges in bichromatic optical lattices,” *Phys. Rev. A* **75**, 063404 (2007).
- ⁷³ Fangzhao Alex An, Eric J. Meier, and Bryce Gadway, “Engineering a flux-dependent mobility edge in disordered zigzag chains,” *Phys. Rev. X* **8**, 031045 (2018).
- ⁷⁴ Dong-Ling Deng, Sriram Ganeshan, Xiaopeng Li, Ranjan Modak, Subroto Mukerjee, and JH Pixley, “Many-body localization in incommensurate models with a mobility edge,” *Annalen der Physik* **529**, 1600399 (2017).
- ⁷⁵ Ranjan Modak and Tanay Nag, “Many-body dynamics in long-range hopping models in the presence of correlated and uncorrelated disorder,” *Phys. Rev. Research* **2**, 012074 (2020).
- ⁷⁶ Archak Purkayastha, Abhishek Dhar, and Manas Kulkarni, “Nonequilibrium phase diagram of a one-dimensional quasiperiodic system with a single-particle mobility edge,” *Phys. Rev. B* **96**, 180204 (2017).
- ⁷⁷ Archak Purkayastha, Sambuddha Sanyal, Abhishek Dhar, and Manas Kulkarni, “Anomalous transport in the aubry-andré-harper model in isolated and open systems,” *Phys. Rev. B* **97**, 174206 (2018).
- ⁷⁸ Ranjan Modak, Soumi Ghosh, and Subroto Mukerjee, “Criterion for the occurrence of many-body localization in the presence of a single-particle mobility edge,” *Phys. Rev. B* **97**, 104204 (2018).
- ⁷⁹ Madhumita Saha, Santanu K. Maiti, and Archak Purkayastha, “Anomalous transport through algebraically localized states in one dimension,” *Phys. Rev. B* **100**, 174201 (2019).
- ⁸⁰ Ranjan Modak and Debraj Rakshit, “Many-body dynamical phase transition in a quasiperiodic potential,” *Phys. Rev. B* **103**, 224310 (2021).
- ⁸¹ Tong Liu, Hao Guo, Yong Pu, and Stefano Longhi, “Gen-

- eralized aubry-andré self-duality and mobility edges in non-hermitian quasiperiodic lattices,” *Physical Review B* **102**, 024205 (2020).
- ⁸² Hui Jiang, Li-Jun Lang, Chao Yang, Shi-Liang Zhu, and Shu Chen, “Interplay of non-hermitian skin effects and anderson localization in nonreciprocal quasiperiodic lattices,” *Physical Review B* **100**, 054301 (2019).
- ⁸³ Quan Lin, Tianyu Li, Lei Xiao, Kunkun Wang, Wei Yi, and Peng Xue, “Topological phase transitions and mobility edges in non-hermitian quasicrystals,” *Physical Review Letters* **129**, 113601 (2022).
- ⁸⁴ Rudolf Gorenflo and Francesco Mainardi, “Random walk models for space-fractional diffusion processes,” (1998).
- ⁸⁵ Supriyo Datta, “Electronic transport in mesoscopic systems,” *Cambridge Studies in Semiconductor Physics and Microelectronic Engineering* (1995), 10.1017/CBO9780511805776.
- ⁸⁶ Eqn. 2-11 have already been derived in Ref⁵ and Ref:⁸⁴. We have incorporated them in our paper for the self-consistency and to improve readability.
- ⁸⁷ J. Biddle, D. J. Priour, B. Wang, and S. Das Sarma, “Localization in one-dimensional lattices with non-nearest-neighbor hopping: Generalized anderson and aubry-andré models,” *Phys. Rev. B* **83**, 075105 (2011).
- ⁸⁸ X. Deng, S. Ray, S. Sinha, G. V. Shlyapnikov, and L. Santos, “One-dimensional quasicrystals with power-law hopping,” *Phys. Rev. Lett.* **123**, 025301 (2019).
- ⁸⁹ Nilanjan Roy and Auditya Sharma, “Fraction of delocalized eigenstates in the long-range aubry-andré-harper model,” *Phys. Rev. B* **103**, 075124 (2021).
- ⁹⁰ Ranjan Modak, Lev Vidmar, and Marcos Rigol, “Quantum adiabatic protocols using emergent local hamiltonians,” *Phys. Rev. E* **96**, 042155 (2017).
- ⁹¹ Philip Richerme, Zhe-Xuan Gong, Aaron Lee, Crystal Senko, Jacob Smith, Michael Foss-Feig, Spyridon Michalakis, Alexey V Gorshkov, and Christopher Monroe, “Non-local propagation of correlations in quantum systems with long-range interactions,” *Nature* **511**, 198–201 (2014).
- ⁹² Petar Jurcevic, Ben P Lanyon, Philipp Hauke, Cornelius Hempel, Peter Zoller, Rainer Blatt, and Christian F Roos, “Quasiparticle engineering and entanglement propagation in a quantum many-body system,” *Nature* **511**, 202–205 (2014).
- ⁹³ Ranjan Modak and Subroto Mukerjee, “Many-body localization in the presence of a single-particle mobility edge,” *Phys. Rev. Lett.* **115**, 230401 (2015).
- ⁹⁴ Dong-Ling Deng, Sriram Ganeshan, Xiaopeng Li, Ranjan Modak, Subroto Mukerjee, and JH Pixley, “Many-body localization in incommensurate models with a mobility edge,” *Annalen der Physik* **529**, 1600399 (2017).
- ⁹⁵ Sabyasachi Nag and Arti Garg, “Many-body mobility edges in a one-dimensional system of interacting fermions,” *Phys. Rev. B* **96**, 060203 (2017).
- ⁹⁶ Zhihao Xu, Xu Xia, and Shu Chen, “Non-hermitian aubry-andré model with power-law hopping,” *Phys. Rev. B* **104**, 224204 (2021).
- ⁹⁷ Ranjan Modak and Bhabani Prasad Mandal, “Eigenstate entanglement entropy in a \mathcal{PT} -invariant non-hermitian system,” *Phys. Rev. A* **103**, 062416 (2021).
- ⁹⁸ Namrata Shukla, Ranjan Modak, and Bhabani Prasad Mandal, “Uncertainty relation for non-hermitian systems,” *Phys. Rev. A* **107**, 042201 (2023).